

RSC Advances



This is an *Accepted Manuscript*, which has been through the Royal Society of Chemistry peer review process and has been accepted for publication.

Accepted Manuscripts are published online shortly after acceptance, before technical editing, formatting and proof reading. Using this free service, authors can make their results available to the community, in citable form, before we publish the edited article. This *Accepted Manuscript* will be replaced by the edited, formatted and paginated article as soon as this is available.

You can find more information about *Accepted Manuscripts* in the [Information for Authors](#).

Please note that technical editing may introduce minor changes to the text and/or graphics, which may alter content. The journal's standard [Terms & Conditions](#) and the [Ethical guidelines](#) still apply. In no event shall the Royal Society of Chemistry be held responsible for any errors or omissions in this *Accepted Manuscript* or any consequences arising from the use of any information it contains.

Influence of the diversified structural variations at the imine functionality of 4-bromophenylacetic acid derived hydrazones on alkaline phosphatase inhibition: Synthesis and molecular modelling studies

Imtiaz Khan^a, Aliya Ibrar^a, Syeda Abida Ejaz^b, Shafi Ullah Khan^b, Syed Jawad Ali Shah^b, Shahid Hameed^{a,*}, Jim Simpson^c, Joanna Lecka^{d,e}, Jean Sévigny^{d,e} and Jamshed Iqbal^{b,*}

^a*Department of Chemistry, Quaid-i-Azam University, Islamabad-45320, Pakistan*

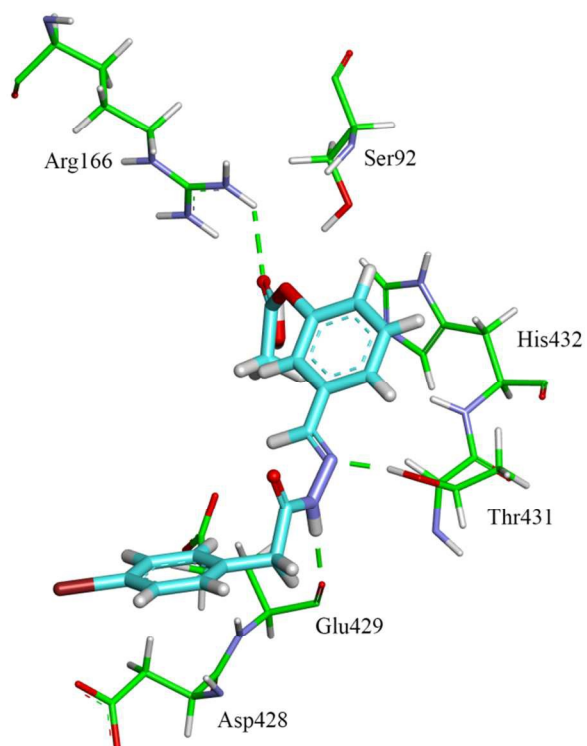
^b*Centre for Advanced Drug Research, COMSATS Institute of Information Technology, Abbottabad-22060, Pakistan*

^c*Department of Chemistry, University of Otago, P.O. Box 56, Dunedin, 9054, New Zealand*

^d*Department of Microbiology-Infectiology and Immunology, Faculty of Medicine, Centre de Recherche du CHU de Québec – Université Laval, Québec, QC, G1V 4G2, Canada*

^e*Centre de Recherche du CHU de Québec – Université Laval, Québec, QC, Canada*

The present study is aimed at developing novel small molecule inhibitors of alkaline phosphatases based on bromophenylacetic acid derived hydrazones.



Putative binding mode of **4g** inside the active pocket of h-PLAP

*Corresponding authors. Tel.: +92-51-9064-2133; Fax: +92-51-9064-2241; E-mail: shameed@gau.edu.pk (S. Hameed); +92-992-383591/96; Fax: +92-992-383441. drjamshed@ciit.net.pk (J. Iqbal)

Abstract

Alkaline phosphatase (AP) isozymes are present in a wide range of species from bacteria to man with an ability to dephosphorylate and transphosphorylate a wide range of substrates. In humans, four AP isozymes have been identified such as tissue-nonspecific (TNAP), intestinal (IAP), placental (PLAP) and germ cell (GCAP) APs. Modulation of activity of the different AP isozymes may have therapeutic implications in distinct diseases and cellular processes. To identify potent inhibitors of APs, a diverse range of 4-bromophenylacetic acid derived hydrazone derivatives has been synthesized and characterized by spectro-analytical methods and, in case of **4i** and **4q**, by single crystal X-ray diffraction analysis. Among the tested series, several compounds were identified as lead candidates showing IC_{50} value from micro to nanomolar range. Compound **4k** displayed an exceptional activity with an IC_{50} value of 10 nM against h-IAP. This inhibitory effect is ~10,000-fold more potent than the standard drug L-phenylalanine. Compounds **4p**, **4g** and **4e** were potent inhibitors of TNAP, PLAP and GCAP, respectively. Molecular docking studies of the respective potent inhibitors have been carried out to rationalize the important binding modes of the most active inhibitors.

Introduction

Alkaline phosphatases (APs, EC 3.1.3.1) are ubiquitous ectoenzymes extensively distributed in nature from bacteria to humans, with the ability to perform important physiological processes. Their main functions comprised of catalyzing dephosphorylation and transphosphorylation reactions on a wide spectrum of physiological and non-physiological substrates.¹⁻³ In humans, four AP isozymes have been identified with differential tissue expression and encoded by distinct genes. These are mainly categorized into two groups: the tissue-specific alkaline phosphatases which include the intestinal (IAP), placental (PLAP), and germ cell (GCAP)

isozymes and the tissue-nonspecific alkaline phosphatase (TNAP), and can be discriminated by their amino acid sequences and their inhibition by specific inhibitors.⁴

TNAP is highly expressed in the developing neural tube, liver and kidney.⁵ Recent and contemporary studies have documented persuasive proof indicating the major role of TNAP in bone tissue hydrolyzing the extra cellular inorganic pyrophosphate, PP_i , to avoid accumulation of this mineralization inhibitor, thereby ensuring normal bone mineralization. Thus, small molecule inhibitors of TNAP have the potential to probe the causative mechanism, or treat disorders of pyrophosphate metabolism such as in generalized arterial calcification of infancy and related rare genetic diseases as well as in chronic kidney disease.⁶

On the other hand, placental alkaline phosphatase (PLAP) is mainly expressed in significant amounts in the syncytiotrophoblast cells of the placenta from about the eighth week of gestation throughout pregnancy.⁷ PLAP was one of the first enzymes recognized as an oncofetal protein expressed in a variety of cancers.⁸ The germ cells alkaline phosphatase (GCAP) is also expressed in the placenta, although at 1/50 the level of PLAP,⁹ but it is expressed in testicular germ cell tumors of the testis, particularly seminomas.¹⁰ PLAP and GCAP are often co-expressed in ovarian cancers,¹¹ and it has been suggested that transformation from normal to malignant trophoblast might be associated with a switch from PLAP to GCAP expression.¹² Moreover, intestinal alkaline phosphatase (IAP) appears to have a role in fat absorption in the gastrointestinal tract,¹³ and as a gut mucosal defense factor,¹⁴ where its expression coincides with the stage of colonization by commensal bacterial flora.¹⁵ Several isozyme-selective inhibitors of APs have been reported (Fig. 1), including L-Phe, L-Trp, L-Leu,¹⁶ and L-homoarginine.¹⁷ Also, levamisole and theophylline are used as TNAP inhibitors.⁶ However, in the recent years, several research groups have identified and optimized small molecule inhibitors of AP isozymes.¹⁸

Hydrazones constitute an important class of biologically active drug molecules which has attracted attention of medicinal chemists due to their wide range of pharmacological properties. These compounds are reported to possess a notable profile of biological actions like antimicrobial, anticonvulsant, antihypertensive, antituberculosis, analgesic, anti-inflammatory, antitumoral, antiglycation, antiproliferative and antimalarial activities.¹⁹ Hydrazones have also been developed as novel inhibitors of IMP-1, a *metallo- β -lactamase*, antioxidant, and antileishmanial agents.²⁰ Moreover, many industrial and biologically active compounds utilize hydrazones as key intermediates for cycloaddition and ring closure reactions.²¹ The attachment of hydrazones has been employed both in the design of ligands for further complexation with transition metals,²² and during the processes of hit-to-lead conversion.²³

We have recently developed chromone-based sulfonamides, diaryl sulfonamides and quinoline-carboxylic acids as potential inhibitors of alkaline phosphatases.²⁴ With this interest, we continued our studies towards the identification of a new class of potent inhibitors of APs, and designed a small molecules library of hydrazone derivatives and showed their successful screening against human recombinant APs. This study identified several potent inhibitory scaffolds targeting various isoforms of APs. To identify the important binding interactions of the most active inhibitors, molecular docking studies were performed.

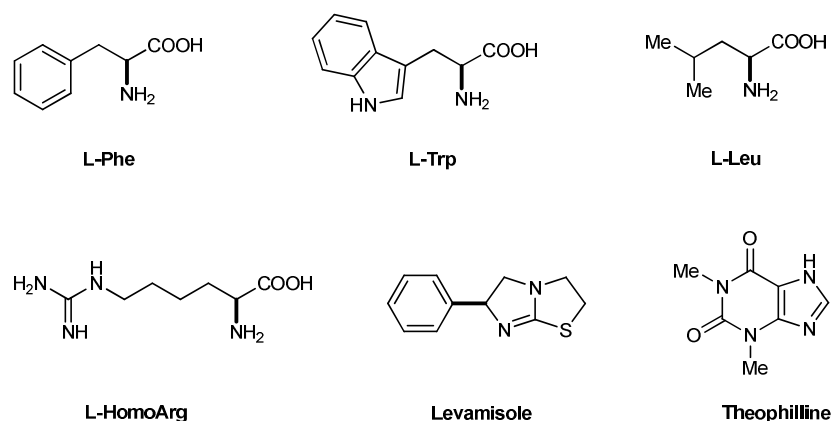


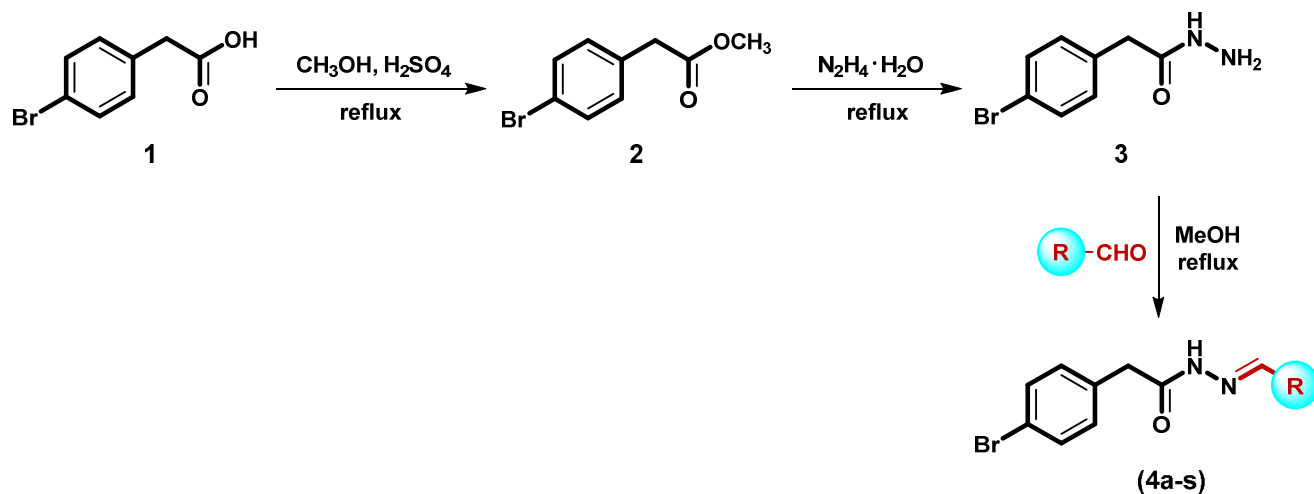
Fig. 1 Examples of AP inhibitors.

Results and discussion

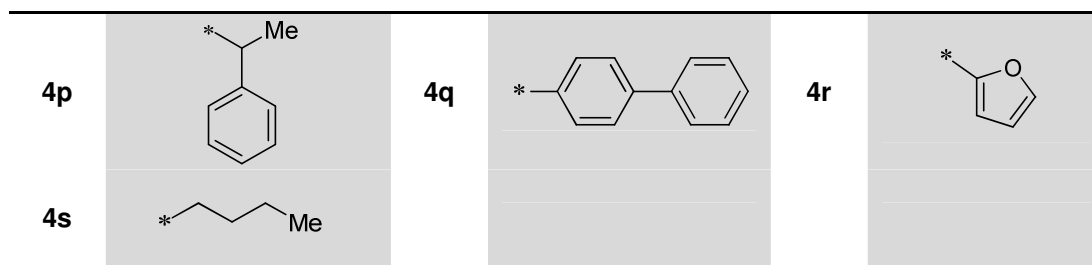
Synthesis of hydrazones

The synthetic route applied for the synthesis of a variety of hydrazone analogues is depicted in Scheme 1. Starting from 4-bromophenylacetic acid (**1**), which was first converted to methyl 2-(4-bromophenyl)acetate (**2**) by heating at reflux in methanol under acidic conditions followed by reaction with hydrazine hydrate to afford 2-(4-bromophenyl)acetohydrazide (**3**).²⁵ Compound **3** was condensed with a range of aldehydes to provide corresponding hydrazones in good yields.²⁶ The scope and generality of this reaction was validated by using a range of aliphatic, aromatic and heteroaromatic aldehydes. A diverse variation of electron-rich ($-\text{OH}$, $-\text{OMe}$, $-\text{OEt}$) and electron-poor ($-\text{NO}_2$) substituents was tolerated on aryl ring of aldehydes producing the desired hydrazones in good yield. However, the aldehyde bearing *para*- NO_2 group gave complex mixture of unidentifiable products. In addition, aldehydes with hydroxyl-protected groups were also used in this condensation reaction affording Schiff bases in excellent yields. Apart from aromatic groups, aldehyde with long chain alkyl group (**4s**) was also tested. Heteroaromatic aldehyde like furfural was also found to be a good coupling partner affording compound **4r** in

85% yield. The reaction involving aldehyde with more sterically demanding biphenyl ring (**4q**) was also taken into account.



Entry	R	Entry	R	Entry	R
4a		4b		4c	
4d		4e		4f	
4g		4h		4i	
4j		4k		4l	
4m		4n		4o	



Scheme 1 Synthesis of hydrazones (**4a–s**).

Characterization of hydrazones

The formation of compounds (**4a–s**) was indicated by their FTIR spectral data where characteristic absorptions were observed in the range of 3218–3171 cm^{-1} attributed to the N–H group in addition to those of C=N in the range of 1650–1582 cm^{-1} . In ^1H NMR spectra, N–H protons resonated in the range of 11.57–11.18 ppm along with additional aromatic protons of the aldehyde moiety. The disappearance of signals for $-\text{NH}_2$ and $-\text{CHO}$ also confirmed the formation of hydrazones. ^{13}C NMR spectra also aided in the confirmation of compounds (**4a–s**) where distinctive signals for imine carbon were observed in the range of 168.9–152.2 ppm. The additional resonances for carbons related to aldehyde coupling partner were also observed in their respective regions with appropriate chemical shift values. ^{13}C NMR spectra were also devoid of aldehyde carbon signals ~ 190 ppm which confirmed the condensation reaction between hydrazide and aldehydes towards the formation of Schiff bases. The purity of the synthesized compounds was ascertained by elemental analysis. For a full structural elucidation, the X-ray diffraction measurements were carried out for the synthesized compounds **4i** and **4q** (see ESI for experimental details). The molecular structures of compounds **4i** and **4q** are illustrated in Fig. 2.

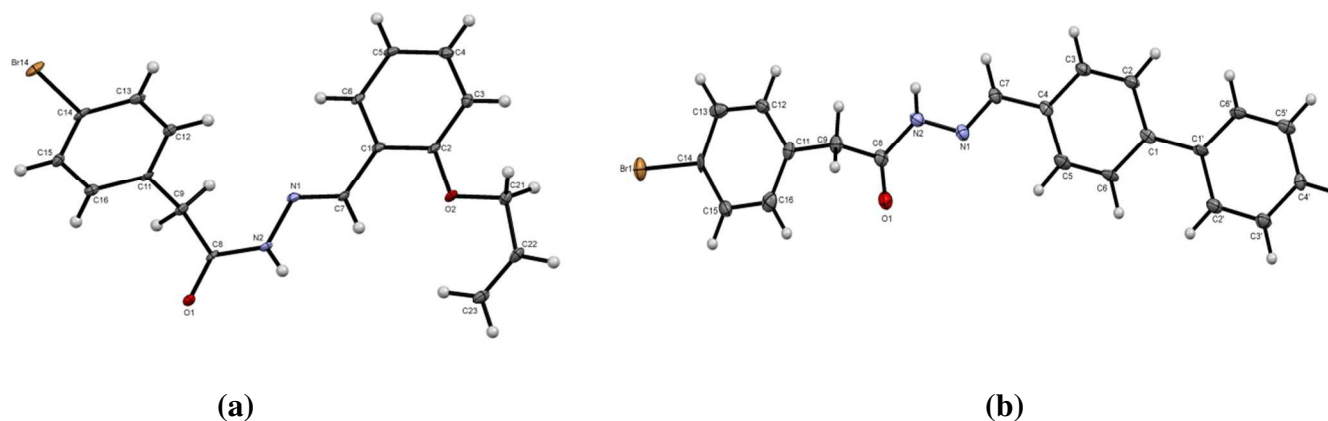


Fig. 2 ORTEP of (a) **4i** and (b) **4q** drawn with 50% ellipsoidal probability along with the atom numbering scheme.

Enzyme inhibition studies

Alkaline phosphatase inhibition

The inhibitory activity potential of the synthesized hydrazones (**4a-s**) against human recombinant APs including TNAP, IAP, PLAP and GCAP was measured using spectrophotometric method.²⁷ The IC_{50} values were determined for compounds which exhibited over 50% inhibition of either of the above mentioned enzymes and the results are presented in Table 1. Levamisole was used as a positive control for both TNAP and PLAP with an IC_{50} value of 25 ± 2 and 120 ± 3 μ M, respectively. Whereas, L-phenylalanine served as a positive control for both IAP and GCAP with an IC_{50} value of 100 ± 3 and 300 ± 5 μ M, respectively. The preliminary data generated from this study led to the identification of **4p**, **4k** and **4g** as the most potent inhibitors of TNAP, IAP and PLAP with IC_{50} values of 0.026 ± 0.001 , 0.01 ± 0.001 and 0.048 ± 0.009 μ M, respectively. Whereas, only compound **4e** inhibited the GCAP with an IC_{50} value of 0.74 ± 0.06 μ M.

Structure-activity relationship analysis

In the light of preliminary data presented in Table 1, a general SAR strategy was developed around the scaffold **4** focusing on the variation of substituents with different nature and number on the aryl ring attached to the imine carbon. In general, among the evaluated hydrazone derivatives, several compounds were identified as potent inhibitors of APs with IC_{50} value ranging from 5 μ M to 10 nM. The incorporation of hydroxyl groups on the phenyl ring generally increased the inhibitory potency up to 27-fold as compared to the standard drug levamisole when tested against h-TNAP (**4a**; $IC_{50} = 0.94 \pm 0.11 \mu$ M). The presence of an *ortho*-hydroxyl group along with the *para*-benzylated hydroxyl group in compound **4c** showed a significant increase in the inhibitory potential which is ~309-fold strong inhibition ($IC_{50} = 0.081 \pm 0.001 \mu$ M). The compounds with hydroxyl groups capped with alkyl or acetyl groups led to a marked reduction in activity (**4d**; 41% inhibition). *Para*-substituent seems essential for activity towards h-TNAP as the data indicates lack of anything in *para*-position shows a large drop in activity (compounds **4e**, **4g** and **4i**).

These compounds also possess benzylated, acetylated and allylated hydroxyl groups at *ortho*- and/*meta*-position of the phenyl ring. On moving the substituent to *para*-position, a marked increase in inhibition potential was noticed. For example, compounds **4h** and **4k** showed ~79- and ~192-fold strong inhibition as compared to the levamisole with IC_{50} values of 0.32 ± 0.002 and $0.13 \pm 0.001 \mu$ M, respectively. Notably, the compounds with *para*-isopropyl (**4l**) and ethoxy (**4m**) group also exhibited potent inhibition of TNAP with IC_{50} values of 0.051 ± 0.006 and $0.23 \pm 0.04 \mu$ M, respectively. This inhibitory potential is ~490- and ~109-fold higher as compared to the standard drug. The introduction of a polarized nitro group on the phenyl ring at *ortho*- and *meta*-position completely eliminates the activity. The most potent compound of this series against TNAP was obtained by introducing an α -branched substituent at the imine carbon. This

derivative (**4p**) displayed ~961-fold increased inhibitory potential with an IC_{50} value of $0.026 \pm 0.001 \mu\text{M}$. Extending the steric bulk by introducing a biphenyl ring or changing the aromatic nature of the substituent afforded compounds **4q** and **4r** with reduced activity. However, the introduction of an alkyl substituent (*n*-Bu) maintained the good inhibition profile with an IC_{50} value of $0.47 \pm 0.02 \mu\text{M}$ which is ~53-fold strong inhibitory efficacy as compared to positive control, levamisole ($IC_{50} = 25 \pm 2 \mu\text{M}$). Overall, from the presented results it could be anticipated that the substituent nature and position on the phenyl ring impart a large impact on the TNAP inhibitory potency.

The synthesized hydrazone analogues were also evaluated against h-IAP using L-phenylalanine as a positive control ($IC_{50} = 100 \pm 3 \mu\text{M}$). On the initial examination of the results it could be noticed that several screened compounds displayed remarkable inhibitory activity ranging from 2.09 μM to 10 nM. In the series, the dihydroxylated compound (**4a**) showed strong inhibitory activity with an IC_{50} value of $0.12 \pm 0.001 \mu\text{M}$ which is ~833-fold higher potential as compared to L-phenylalanine. The variation of the substituent position and nature of hydroxyl protecting groups decreased the potency but still these compounds showed a beneficial effect by inhibiting h-IAP with a better ability as compared to the standard drug. These compounds (**4c** and **4d**) were potent inhibitors with ~48- and ~625-fold higher potency. The compounds with *ortho*-benzylated (**4e**), *para*-acetylated (**4h**), and *ortho*-allylated (**4i**) hydroxyl groups showed less than 50% inhibition. However, the compound (**4g**) with a *meta*-acetylated hydroxyl group displayed ~312-fold strong inhibition strength with an $IC_{50} = 0.32 \pm 0.04 \mu\text{M}$, whereas, **4k** bearing a *para*-allylated hydroxyl substituent emerged as the most potent analogue showing an exceptional activity with an IC_{50} value of 10 nM. This inhibitory effect is ~10,000-fold stronger as compared to the standard drug L-phenylalanine. Also, this compound is the lead member of the evaluated

series. Steric bulk was unfavorable for activity in addition to the electron-withdrawing groups on the aryl ring. Also, the compounds with hetero-aromatic (**4r**) and aliphatic (**4s**) substituents were not suitable candidates for h-IAP inhibition. However, compound **4m** incorporating an electron-donating (-OEt) group inhibited the IAP with ~170-fold enhanced efficacy.

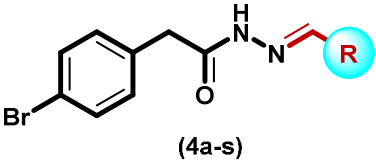
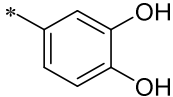
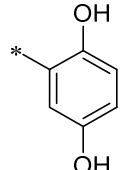
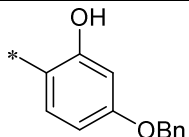
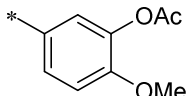
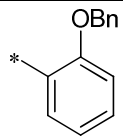
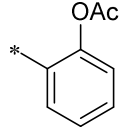
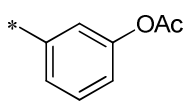
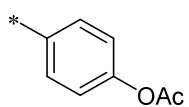
Similarly, the synthesized hydrazone derivatives were also tested against h-PLAP, another isozyme of the alkaline phosphatase family. Several compounds showed an excellent inhibition results. The activity data is summarized in Table 1. The compound **4a** with free hydroxyl groups inhibited the PLAP enzyme with ~222-fold better efficacy and displayed an IC_{50} value of $0.54 \pm 0.03 \mu\text{M}$. Also, the compounds **4c** and **4d** with free or protected hydroxyl groups at variable positions showed a good inhibition profile with an IC_{50} value of 0.36 ± 0.01 and $0.26 \pm 0.01 \mu\text{M}$, respectively. These results demonstrated the strong inhibitory action of compounds **4a** and **4d** against PLAP which is ~333- and ~461-fold, respectively. Similar to the previous results, *ortho*-benzylated product could not inhibit the PLAP with better efficiency. However, the compound with a *meta*-acetylated hydroxyl group (**4g**) demonstrated the highest inhibitory potential against PLAP among the tested compounds. This compound showed an IC_{50} value of $0.048 \pm 0.009 \mu\text{M}$ which is ~2500-fold strong inhibition potential. On moving the substituent from *meta*- to *para*-position afforded compound **4h** with reduced activity but still this inhibition is ~107-fold higher as compared to levamisole. Compounds with *ortho*- and *para*-allylated hydroxyl (**4i** and **4k**) groups were also potent inhibitors where **4k** inhibited PLAP more strongly (~4-fold) as compared to **4i** and ~2033-fold as compared to positive control. The compounds with *para*-substituents like **4l** and **4m** maintained a similar trend of inhibition by inhibiting PLAP with ~293-fold ($IC_{50} = 0.41 \pm 0.01 \mu\text{M}$) and ~1428-fold ($IC_{50} = 0.084 \pm 0.001 \mu\text{M}$), respectively. In contrast to the previous results, the compounds (**4n** and **4o**) incorporating electron-deficient (-

NO₂) group at *ortho*- and *meta*-positions of the phenyl ring attached to the imine carbon exhibited remarkable inhibitory potential against PLAP with an IC₅₀ value of 0.066 ± 0.003 and 0.23 ± 0.06 μM, respectively. In this case, the *ortho*-substituted derivative (**4n**) was 3- and 1818-fold superior as compared to **4o** and levamisole, respectively, in terms of inhibition results. The incorporation of an additional carbon unit spacer between the phenyl ring and the imine moiety produced compound **4p** which exhibited ~24-fold strong inhibition (IC₅₀ = 5.04 ± 0.94 μM). The introduction of a heterocyclic moiety such as furanyl (**4r**) resulted in a significant inhibition of PLAP with an IC₅₀ value of 0.14 ± 0.02 μM. This potential is ~857-fold higher as compared to the levamisole and is in contrast with the inhibition data of this compound against TNAP and IAP where less than 50% inhibition has been observed. Compound **4s** with an alkyl group also demonstrated excellent inhibition potential with ~222-fold better efficacy (IC₅₀ = 0.54 ± 0.01 μM).

The synthesized compounds were also tested for their inhibitory potential against h-GCAP where only **4e** incorporating *ortho*-benzylated hydroxyl group emerged as a significantly potent and lead member with an IC₅₀ value of 0.74 ± 0.06 μM. This inhibition is ~405-fold strong as compared to the L-phenylalanine (IC₅₀ = 300 ± 5 μM) and is in contrast with the previous results obtained for this compound against other isozymes of alkaline phosphatase such as TNAP, IAP and PLAP. The rest of the compounds showed less than 50% inhibition.

To sum up, these data clearly demonstrate that the nature of the substituent and the position on the phenyl ring are the main and critical factors determining the potency (and selectivity) for the inhibition of the various isoforms of alkaline phosphatase.

Table 1. ALP inhibition data for hydrazones (4a-s)

 (4a-s)					
Compounds	Substituent (R)	Alkaline phosphatase inhibition			
		h-TNAP	h-IAP	h-PLAP	h-GCAP
		IC ₅₀ ± SEM (μM) / %inhibition			
Levamisole	—	25 ± 2	—	120 ± 3	—
L-Phenylalanine	—	—	100 ± 3	—	300 ± 5
4a		0.94 ± 0.11	0.12 ± 0.001	0.54 ± 0.03	28.8%
4b		—	—	—	—
4c		0.081 ± 0.001	2.09 ± 0.78	0.36 ± 0.01	11.2%
4d		41.2%	0.16 ± 0.02	0.26 ± 0.01	7.28%
4e		43.8%	42.8%	44.8%	0.74 ± 0.06
4f		—	—	—	—
4g		42.1%	0.32 ± 0.04	0.048 ± 0.009	36.7%
4h		0.32 ± 0.002	46.1%	1.12 ± 0.013	33.2%

4i		38.2%	33.2%	0.21 ± 0.02	41.9%
4j		—	—	—	—
4k		0.13 ± 0.001	0.01 ± 0.001	0.059 ± 0.003	45.7%
4l		0.051 ± 0.006	37.5%	0.41 ± 0.01	21.5%
4m		0.23 ± 0.04	0.59 ± 0.03	0.084 ± 0.001	38.7%
4n		38.9%	36.8%	0.066 ± 0.003	44.9%
4o		43.6%	29.7%	0.23 ± 0.06	23.6%
4p		0.026 ± 0.001	47.2%	5.04 ± 0.94	33.5%
4q		37.1%	44.1%	36.3%	34.8%
4r		41.4%	41.2%	0.14 ± 0.002	24.6%
4s		0.47 ± 0.02	31.2%	0.54 ± 0.01	23.8%

The IC₅₀ is the concentration at which 50% of the enzyme activity is inhibited. The % inhibition is the value that compound inhibits specific isozyme at 200 μM concentration. The values are reported with standard error of mean (IC₅₀ ± SEM). The experiments were performed in triplicate, n = 3 (See method for detail).

Homology modelling and molecular docking studies

Homology models of human derived tissue non-specific and intestinal alkaline phosphatase was performed previously²⁴ and is used for molecular docking of our compounds. However, homology modelling for h-GCAP was carried out using Modeller v9.14²⁸ via Chimera v1.10.1.²⁹ Basic Local Alignment Search Tool (BLAST) of NCBI protein database identified crystal structure of human derived placental alkaline phosphatase as top ranking templates and PDB ID 1ZED was thus used for modelling because of its high percentage identity with human germ cell alkaline phosphatase (i.e. 97.7% identity). Five homology models were generated. The Ramachandran plot of the homology model shows good stereochemical quality of the model with 97.72% residues in favored region and only 0.21% as Ramachandran outliers (see ESI for details).

The active site analysis of the human derived germ cells alkaline phosphatase with its template protein structure revealed only a single amino acid residue change from amino acid Glu429 (of h-PLAP) to amino acid Gly429 (inside h-GCAP). All other amino acids of the active pocket are highly conserved (see ESI for details).

Molecular docking studies were performed to rationalize the most plausible binding modes of APs inhibitors. Docking studies were carried out for the most active inhibitors against specific AP isoenzymes. These compounds oriented themselves in a similar pattern inside the APs active site. However, for each active compound inside their respective isozyme the individual interactions in some cases were observed, while in other cases some interaction differs. This difference in individual interaction is either due to the presence or absence of specific functional groups present in individual active compound or due to the difference in the amino acid makeup of the individual isozyme.

The compound **4g** inside the h-PLAP forms characteristic hydrogen bonding interaction with Arg166, Thr431 and with Glu429 and is in compliance with previously reported interactions.³⁰ Substitution of phenyl acetate in case of compound **4g** was proved to be more favorable inside the active pocket of h-PLAP by providing as extra carbonyl functional group that can form additional hydrogen bonding interactions with amino acid Arg166 and possible interaction with Ser92.

Similar to compound **4g**, almost similar binding mode was determined for compound **4k** inside h-IAP i.e., hydrogen bonding interaction was observed with amino acid Arg166 and Thr431. Unlike compound **4g** hydrogen bonding interaction occurs with Ser429 (specific amino acid of h-IAP instead of amino acid residue Glu429 of h-PLAP). *p*-Allyloxybenzene substitution in case of compound **4k** was found to be oriented deep in the active site groove of h-IAP and oxygen moiety of this substitution is responsible for the interaction of compound with amino acid Arg166, however the catalytic amino acid Ser92 was found to be little farther away to form any interaction with compound **4k**.

Molecular docking of ethylbenzene substituted compound **4p** inside the h-TNAP yields interactions similar to that of compound **4g**, i.e. it forms hydrogen bonding interactions with amino acid residue Thr437. Unlike compound **4g**, where the h-PLAP specific amino acid Glu429 is involved in hydrogen bonding interaction with protonated nitrogen of compound **4g**, no such interaction was observed because of h-TNAP basic amino acid residue His434. However, amino acid His434 was observed to form a Pi-Pi stacking interaction with bromobenzene of compound **4p**. Other interaction such as interaction with amino acid His437 and Glu435 was also observed. Except interaction with amino acid Arg167 all these interaction are similar to interactions previously reported.²⁴ Ethylbenzene substituted group in case of compound **4p** was oriented in

direction opposite to that of earlier substitution of **4g** or **4k** due to hydrophobic nature of the substitution and thus no interaction with amino acid Arg167 was observed.

Molecular docking of compound **4e** also revealed poses similar to other compounds (**4g**, **4k** and **4p**). Similar to the compound **4g**, a hydrogen bonding interaction of amino acid Thr431 with carbonyl moiety of the compound was observed. The benzyloxybenzene substitution of the compound **4e** aligned itself in such a way that its oxygen moiety forms polar interaction with amino acid His432. Additionally, imidazole ring of amino acid His432 forms a Pi-Pi stacking interaction with the benzene of benzyloxy substitution of compound **4e** and thus, stabilized the pose. The molecular docking interactions of the most active compounds **4e**, **4g**, **4k** and **4p** inside h-GCAP, h-PLAP, h-IAP and h-TNAP respectively, can be seen in Fig. 3.

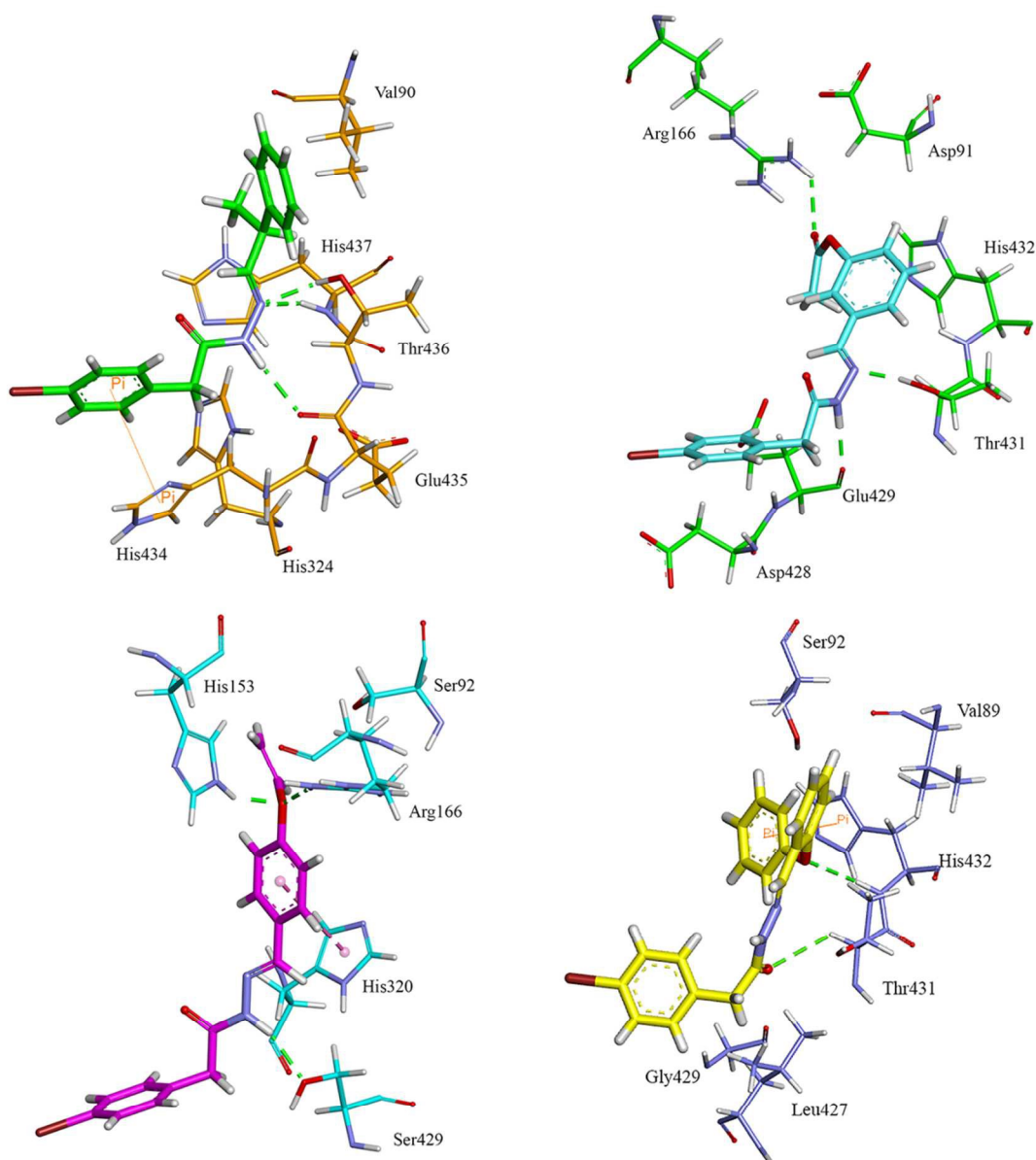


Fig. 3 Putative binding mode of compound **4p** (colored green) inside h-TNAP model (amino acid colored brown), compound **4g** (colored light blue) inside h-PLAP (amino acid colored green), compound **4k** (colored magenta) inside h-IAP (amino acid colored cyan) and compound **4e** (colored yellow) inside h-GCAP (colored blue).

Conclusions

In summary, a series of hydrazone derivatives (**4a-s**) based on 4-bromophenyl acetic acid was designed and synthesized with a diverse range of substituents at the imine functionality. The resulting compounds were established on the basis of spectro-analytical data and, in case of **4i** and **4q**, by X-ray crystallography. The synthesized compounds displayed alkaline phosphatase inhibition in low nanomolar to micromolar range and several compounds were identified as lead candidates. Compound **4k** displayed an exceptional activity with an IC_{50} value of 10 nM against h-IAP with a strong inhibitory effect of ~10,000-fold as compared to the standard drug L-phenylalanine. Compounds **4p**, **4g** and **4e** were potent inhibitors of human TNAP, PLAP and GCAP, respectively. Molecular docking studies results revealed the important interactions between the most active inhibitors and specific APs isoenzymes. The presented SAR and the identified inhibitors provide an excellent platform for further optimization of AP inhibitors.

Experimental

Materials and methods

Unless specified otherwise, all commercially available reagents and solvents were used as received. Thin layer chromatography (TLC) was performed on Merck DF-Alufoilien 60F₂₅₄ 0.2 mm precoated plates. Compounds were visualized by exposure to UV light at 254 and 365 nm. Melting points were recorded on a Stuart melting point apparatus (SMP3) and are uncorrected. Infra-red (IR) spectra were recorded on FTS 3000 MX, Bio-Rad Merlin (Excalibur model) spectrophotometer. NMR spectra were acquired on Bruker AV300 spectrometer at room temperature unless otherwise stated. ¹H and ¹³C NMR spectra were referenced to external tetramethylsilane *via* the residual protonated solvent (¹H) or the solvent itself (¹³C). All chemical shifts are reported in parts per million (ppm). For (CD₃)₂SO, the shifts are referenced to 2.50

ppm for ^1H NMR spectroscopy and 39.52 ppm for ^{13}C NMR spectroscopy. Abbreviations used in the description of resonances are: s (singlet), br s (broad singlet), d (doublet), dd (doublet of doublet), t (triplet), q (quartet), m (multiplet), Ar (aromatic). The elemental analysis was performed on Leco CHNS-932 Elemental Analyzer, Leco Corporation (USA).

Preparation of hydrazones (4a-s)

Preparation of 2-(4-bromophenyl)acetohydrazide (3)

The synthesis of 2-(4-bromophenyl)acetohydrazide (**3**) was accomplished according to a literature reported procedure.²⁵ The data was found to be consistent with those observed previously.³¹

General procedure for the preparation of hydrazone derivatives (4a-s)

To a stirred solution of 2-(4-bromophenyl)acetohydrazide (**3**) (1.0 mmol) in methanol was added appropriate aldehyde (1.2 mmol) and the reaction mixture was heated at reflux for 7 h. After completion of the reactions (monitored by TLC analysis), the reaction mixture was cooled to room temperature. The excess solvent was removed under reduced pressure and the purification of the residue by recrystallization (30% acetone/hexane) afforded the desired hydrazone derivatives (**4a-s**).²⁶

2-(4-Bromophenyl)-N'-(3,4-dihydroxybenzylidene)acetohydrazide (4a)

The general experimental procedure described above afforded **4a** as a light brown solid (81%, 289 mg). m.p 217-218 °C; R_f : 0.76 (10% MeOH/ CHCl_3); IR (ATR, cm^{-1}): 3444 (OH), 3243 (NH), 3063 (Ar-H), 1645 (C=O), 1594 (C=N), 1547, 1520 (C=C); ^1H NMR (300 MHz, $\text{DMSO-}d_6$): δ 11.18 (s, 1H, NH), 9.15 (s, 1H, OH), 8.01 (s, 2H, OH, C-H), 7.52-7.48 (m, 3H, Ar-H), 7.28-7.17 (m, 2H, Ar-H), 6.82 (dd, 2H, $J = 8.1, 7.2$, Ar-H), 3.93 (s, 2H, CH_2); ^{13}C NMR (75 MHz, $\text{DMSO-}d_6$): δ 171.9, 166.2, 148.4, 148.2, 135.8, 132.2, 131.8, 131.6, 131.5, 126.1, 121.0,

120.2, 44.2. Analysis Calcd. for $C_{15}H_{13}BrN_2O_3$ (348.01): C, 51.60; H, 3.75; N, 8.02. Found: C, 51.42; H, 3.69; N, 7.91.

2-(4-Bromophenyl)-N'-(2,4-dihydroxybenzylidene)acetohydrazide (4b)

The general experimental procedure described above afforded **4b** as a brown solid (70%, 250 mg). m.p 201-202 °C; R_f : 0.73 (10% MeOH/ $CHCl_3$); IR (ATR, cm^{-1}): 3424 (OH), 3198 (NH), 3053 (Ar-H), 1637 (C=O), 1580 (C=N), 1574, 1523 (C=C); 1H NMR (300 MHz, DMSO- d_6): δ 11.07 (s, 1H, NH), 9.28 (s, 1H, OH), 7.76 (s, 2H, OH, C-H), 7.56-7.40 (m, 3H, Ar-H), 7.37-7.21 (m, 2H, Ar-H), 6.87-6.73 (m, 2H, Ar-H), 3.90 (s, 2H, CH_2); ^{13}C NMR (75 MHz, DMSO- d_6): δ 170.8, 165.0, 146.1, 139.6, 134.9, 131.5, 130.7, 130.1, 129.5, 127.0, 122.3, 120.4, 45.6. Analysis Calcd. for $C_{15}H_{13}BrN_2O_3$ (348.01): C, 51.60; H, 3.75; N, 8.02. Found: C, 51.48; H, 3.67; N, 7.85.

N'-(4-(Benzyloxy)-2-hydroxybenzylidene)-2-(4-bromophenyl)acetohydrazide (4c)

The general experimental procedure described above afforded **4c** as a white solid (79%, 346 mg). m.p 200-201 °C; R_f : 0.73 (10% MeOH/ $CHCl_3$); IR (ATR, cm^{-1}): 3440 (OH), 3187 (NH), 3065 (Ar-H), 1662 (C=O), 1627 (C=N), 1605, 1566 (C=C); 1H NMR (300 MHz, DMSO- d_6): δ 11.40 (s, 1H, NH), 10.23 (s, 1H, OH), 8.32 (s, 1H, C-H), 8.20 (s, 1H, Ar-H), 7.60-7.23 (m, 8H, Ar-H), 6.59-6.53 (m, 3H, Ar-H), 5.11 (s, 2H, OCH_2), 3.91 (s, 2H, CH_2); ^{13}C NMR (75 MHz, DMSO- d_6): δ 171.6, 166.2, 158.3, 148.1, 141.9, 137.2, 135.4, 132.1, 131.9, 131.6, 131.5, 128.9, 128.4, 128.2, 120.3, 113.7, 69.8, 44.3. Analysis Calcd. for $C_{22}H_{19}BrN_2O_3$ (438.06): C, 60.15; H, 4.36; N, 6.38. Found: C, 59.98; H, 4.47; N, 6.24.

N'-(3-(Acetoxy)-4-methoxybenzylidene)-2-(4-bromophenyl)acetohydrazide (4d)

The general experimental procedure described above afforded **4d** as a light yellow solid (83%, 335 mg). m.p 198-199 °C; R_f : 0.73 (10% MeOH/ $CHCl_3$); IR (ATR, cm^{-1}): 3195 (NH), 3068 (Ar-H), 1667 (C=O), 1650 (C=N), 1591, 1488 (C=C); 1H NMR (300 MHz, DMSO- d_6): δ 11.51 (s,

1H, NH), 8.20 (s, 1H, C-H), 7.97 (s, 1H, Ar-H), 7.53-7.48 (m, 2H, Ar-H), 7.28 (d, 2H, $J = 8.4$ Hz, Ar-H), 7.17-7.13 (m, 2H, Ar-H), 3.99 (s, 3H, OCH₃), 3.55 (s, 2H, CH₂), 2.27 (s, 3H, CH₃); ¹³C NMR (75 MHz, DMSO-*d*₆): δ 172.5, 168.9, 166.7, 151.6, 146.5, 140.9, 133.6, 131.8, 131.6, 131.5, 123.7, 120.8, 120.3, 56.3, 40.9, 20.9. Analysis Calcd. for C₁₈H₁₇BrN₂O₄ (404.04): C, 53.35; H, 4.23; N, 6.91. Found: C, 53.12; H, 4.47; N, 6.79.

***N'*-(2-(Benzyloxy)benzylidene)-2-(4-bromophenyl)acetohydrazide (4e)**

The general experimental procedure described above afforded **4e** as a white solid (78%, 329 mg). m.p 170-171 °C; R_f: 0.75 (10% MeOH/CHCl₃); IR (ATR, cm⁻¹): 3187 (NH), 3069 (Ar-H), 1661 (C=O), 1597 (C=N), 1541, 1487 (C=C); ¹H NMR (300 MHz, DMSO-*d*₆): δ 11.48 (s, 1H, NH), 8.49 (s, 1H, C-H), 7.91-7.83 (m, 2H, Ar-H), 7.52-7.46 (m, 2H, Ar-H), 7.45-7.31 (m, 2H, Ar-H), 7.29-7.26 (m, 2H, Ar-H), 7.18 (d, 2H, $J = 8.4$ Hz, Ar-H), 7.08-6.97 (m, 3H, Ar-H), 5.18 (s, 2H, OCH₂), 3.97 (s, 2H, CH₂); ¹³C NMR (75 MHz, DMSO-*d*₆): δ 172.2, 166.4, 157.1, 142.2, 139.3, 137.2, 136.9, 135.7, 135.6, 132.2, 131.8, 131.6, 131.5, 129.0, 120.3, 120.3, 70.1, 44.6. Analysis Calcd. for C₂₂H₁₉BrN₂O₂ (422.06): C, 62.42; H, 4.52; N, 6.62. Found: C, 62.31; H, 4.39; N, 6.71.

2-((2-(2-(4-Bromophenyl)acetyl)hydrazono)methyl)phenyl acetate (4f)

The general experimental procedure described above afforded **4f** as an off-white solid (71%, 265 mg). m.p 181-182 °C; R_f: 0.69 (10% MeOH/CHCl₃); IR (ATR, cm⁻¹): 3172 (NH), 3057 (Ar-H), 1750, 1639 (C=O), 1600 (C=N), 1560, 1490 (C=C); ¹H NMR (300 MHz, DMSO-*d*₆): δ 11.17 (s, 1H, NH), 8.57 (s, 1H, C-H), 7.80-7.77 (m, 4H, Ar-H), 7.63-7.56 (m, 4H, Ar-H), 3.72 (s, 2H, CH₂), 2.33 (s, 3H, CH₃); ¹³C NMR (75 MHz, DMSO-*d*₆): δ 171.4, 167.2, 153.2, 144.0, 139.1, 134.8, 131.8, 131.4, 131.1, 130.4, 129.0, 127.6, 126.9, 45.7, 25.1. Analysis Calcd. for C₁₇H₁₅BrN₂O₃ (374.03): C, 54.42; H, 4.03; N, 7.47. Found: C, 54.05; H, 3.91; N, 7.35.

3-((2-(2-(4-Bromophenyl)acetyl)hydrazono)methyl)phenyl acetate (4g)

The general experimental procedure described above afforded **4g** as an off-white solid (75%, 280 mg). m.p 197-198 °C; R_f : 0.76 (10% MeOH/CHCl₃); IR (ATR, cm⁻¹): 3192 (NH), 3065 (Ar-H), 1755, 1645 (C=O), 1607 (C=N), 1578, 1485 (C=C); ¹H NMR (300 MHz, DMSO-*d*₆): δ 11.29 (s, 1H, NH), 8.61 (s, 1H, C-H), 7.99-7.90 (m, 3H, Ar-H), 7.84-7.77 (m, 3H, Ar-H), 7.66-7.59 (m, 2H, Ar-H), 3.87 (s, 2H, CH₂), 2.30 (s, 3H, CH₃); ¹³C NMR (75 MHz, DMSO-*d*₆): δ 171.0, 166.8, 151.6, 140.5, 138.5, 132.1, 131.9, 131.7, 131.6, 130.3, 128.7, 127.9, 127.6, 43.5, 24.0. Analysis Calcd. for C₁₇H₁₅BrN₂O₃ (374.03): C, 54.42; H, 4.03; N, 7.47. Found: C, 54.25; H, 4.27; N, 7.37.

4-((2-(2-(4-Bromophenyl)acetyl)hydrazono)methyl)phenyl acetate (4h)

The general experimental procedure described above afforded **4h** as a yellow solid (77%, 288 mg). m.p 207-208°C; R_f : 0.68 (10% MeOH/CHCl₃); IR (ATR, cm⁻¹): 3218 (NH), 3068 (Ar-H), 1726, 1661 (C=O), 1594 (C=N), 1557, 1513 (C=C); ¹H NMR (300 MHz, DMSO-*d*₆): δ 11.40 (s, 1H, NH), 8.34 (s, 1H, C-H), 7.80-7.71 (m, 2H, Ar-H), 7.62-7.54 (m, 2H, Ar-H), 7.45-7.33 (m, 2H, Ar-H), 7.19-7.14 (m, 2H, Ar-H), 3.92 (s, 2H, CH₂), 2.30 (s, 3H, CH₃); ¹³C NMR (75 MHz, DMSO-*d*₆): δ 171.4, 166.7, 159.4, 140.2, 138.2, 132.7, 132.2, 131.7, 131.6, 127.1, 125.9, 44.5, 28.5. Analysis Calcd. for C₁₇H₁₅BrN₂O₃ (374.03): C, 54.42; H, 4.03; N, 7.47. Found: C, 54.21; H, 4.32; N, 7.29.

N'-(2-(Allyloxy)benzylidene)-2-(4-bromophenyl)acetohydrazide (4i)

The general experimental procedure described above afforded **4i** as a light brown solid (77%, 286 mg). m.p 176-177 °C; R_f : 0.72 (10% MeOH/CHCl₃); IR (ATR, cm⁻¹): 3171 (NH), 3074 (Ar-H), 1667 (C=O), 1609 (C=N), 1573, 1519 (C=C); ¹H NMR (300 MHz, DMSO-*d*₆): δ 11.45 (s, 1H, NH), 8.59 (s, 1H, C-H), 7.88-7.79 (m, 1H, Ar-H), 7.52-7.47 (m, 2H, Ar-H), 7.39-7.24 (m, 3H, Ar-H), 7.15-6.96 (m, 2H, Ar-H), 6.11-6.00 (m, 1H, C-H), 5.50-5.44 (m, 1H, C-H), 5.32-5.26 (m, 1H, C-H), 4.63 (br s, 2H, OCH₂), 3.97 (s, 2H, CH₂); ¹³C NMR (75 MHz, DMSO-*d*₆): δ

158.2, 157.0, 156.9, 142.4, 139.3, 135.7, 133.7, 132.2, 131.6, 131.5, 126.0, 125.8, 121.4, 117.6, 69.0, 38.8. Analysis Calcd. for $C_{18}H_{17}BrN_2O_2$ (372.05): C, 57.92; H, 4.59; N, 7.51. Found: C, 57.88; H, 4.68; N, 7.46.

***N'*-(3-(Allyloxy)benzylidene)-2-(4-bromophenyl)acetohydrazide (4j)**

The general experimental procedure described above afforded **4j** as a brown solid (70%, 260 mg). m.p 165-166 °C; R_f : 0.68 (10% MeOH/ $CHCl_3$); IR (ATR, cm^{-1}): 3155 (NH), 3067 (Ar-H), 1660 (C=O), 1622 (C=N), 1569, 1524 (C=C); 1H NMR (300 MHz, $DMSO-d_6$): δ 11.40 (s, 1H, NH), 8.48 (s, 1H, C-H), 7.80-7.72 (m, 1H, Ar-H), 7.50-7.44 (m, 2H, Ar-H), 7.37-7.28 (m, 3H, Ar-H), 7.21-6.99 (m, 2H, Ar-H), 6.18-6.08 (m, 1H, C-H), 5.54-5.48 (m, 1H, C-H), 5.30-5.26 (m, 1H, C-H), 4.69 (br s, 2H, OCH_2), 3.92 (s, 2H, CH_2); ^{13}C NMR (75 MHz, $DMSO-d_6$): δ 159.1, 157.8, 155.7, 144.1, 140.2, 136.4, 133.7, 132.6, 131.9, 131.3, 128.4, 126.2, 123.8, 119.5, 68.7, 39.7. Analysis Calcd. for $C_{18}H_{17}BrN_2O_2$ (372.05): C, 57.92; H, 4.59; N, 7.51. Found: C, 57.79; H, 4.50; N, 7.38.

***(E)*-*N'*-(4-(Allyloxy)benzylidene)-2-(4-bromophenyl)acetohydrazide (4k)**

The general experimental procedure described above afforded **4k** as a yellow solid (74%, 265 mg). m.p 140-141 °C; R_f : 0.74 (10% MeOH/ $CHCl_3$); IR (ATR, cm^{-1}): 3218 (NH), 3071 (Ar-H), 1666 (C=O), 1622 (C=N), 1600, 1573, 1505 (C=C); 1H NMR (300 MHz, $DMSO-d_6$): δ 11.54 (s, 1H, NH), 8.43 (s, 1H, C-H), 7.97-7.82 (m, 2H, Ar-H), 7.78-7.62 (m, 2H, Ar-H), 7.54-7.33 (m, 4H, Ar-H), 6.95-6.79 (m, 1H, C-H), 6.14-5.97 (m, 2H, CH_2), 5.56 (m, 2H, OCH_2), 3.89 (s, 2H, CH_2); ^{13}C NMR (75 MHz, $DMSO-d_6$): δ 172.2, 158.2, 141.6, 139.2, 132.7, 132.2, 131.7, 131.4, 130.6, 127.9, 126.1, 125.3, 65.7, 45.3. Analysis Calcd. for $C_{18}H_{17}BrN_2O_2$ (358.07): C, 57.92; H, 4.59; N, 7.51. Found: C, 57.74; H, 4.35; N, 7.37.

2-(4-Bromophenyl)-*N'*-(4-isopropylbenzylidene)acetohydrazide (4l)

The general experimental procedure described above afforded **4l** as a yellow solid (73%, 261 mg). m.p 149-150 °C; R_f : 0.70 (10% MeOH/CHCl₃); IR (ATR, cm⁻¹): 3194 (NH), 3033 (Ar-H), 1652 (C=O), 1607 (C=N), 1572, 1504 (C=C); ¹H NMR (300 MHz, DMSO-*d*₆): δ 11.31 (s, 1H, NH), 8.37 (s, 1H, C-H), 7.90-7.86 (m, 2H, Ar-H), 7.78-7.64 (m, 2H, Ar-H), 7.59-7.46 (m, 2H, Ar-H), 6.99-6.84 (m, 2H, Ar-H), 2.86-2.78 (m, 1H, C-H), 2.26 (d, 6H, *J* = 6.9 Hz, CH₃), 3.83 (s, 2H, CH₂); ¹³C NMR (75 MHz, DMSO-*d*₆): δ 171.3, 156.7, 140.2, 132.8, 132.1, 131.6, 131.4, 130.6, 126.4, 124.9, 46.7, 44.2, 29.7. Analysis Calcd. for C₁₈H₁₉BrN₂O (358.07): C, 60.18; H, 5.33; N, 7.80. Found: C, 60.22; H, 5.17; N, 7.66.

2-(4-Bromophenyl)-N'-(4-ethoxybenzylidene)acetohydrazide (4m)

The general experimental procedure described above afforded **4m** as an off-white solid (83%, 299 mg). m.p 160-161 °C; R_f : 0.72 (10% MeOH/CHCl₃); IR (ATR, cm⁻¹): 3181 (NH), 3085 (Ar-H), 1661 (C=O), 1598 (C=N), 1547, 1518 (C=C); ¹H NMR (300 MHz, DMSO-*d*₆): δ 11.23 (s, 1H, NH), 8.57 (s, 1H, C-H), 8.05-8.02 (m, 2H, Ar-H), 7.53-7.47 (m, 2H, Ar-H), 7.40-7.33 (m, 2H, Ar-H), 7.30-7.25 (m, 2H, Ar-H), 5.12 (q, 2H, *J* = 6.9 Hz, OCH₂), 3.87 (s, 2H, CH₂), 1.34 (t, 3H, *J* = 6.6 Hz, CH₃); ¹³C NMR (75 MHz, DMSO-*d*₆): δ 170.3, 158.6, 139.8, 134.6, 132.4, 131.8, 131.5, 131.4, 130.1, 126.4, 55.9, 39.7, 28.4. Analysis Calcd. for C₁₇H₁₇BrN₂O₂ (360.05): C, 57.92; H, 4.59; N, 7.51. Found: C, 57.86; H, 4.38; N, 7.42.

N'-(2-Nitrobenzylidene)-2-(4-bromophenyl)acetohydrazide (4n)

The general experimental procedure described above afforded **4n** as an off-white solid (75%, 271 mg). m.p 239-240 °C; R_f : 0.78 (10% MeOH/CHCl₃); IR (ATR, cm⁻¹): 3181 (NH), 3075 (Ar-H), 1665 (C=O), 1582 (C=N), 1529, 1514 (C=C); ¹H NMR (300 MHz, DMSO-*d*₆): δ 11.57 (s, 1H, NH), 8.09 (s, 1H, C-H), 7.89-7.82 (m, 2H, Ar-H), 7.53-7.47 (m, 2H, Ar-H), 7.27-7.23 (m, 2H, Ar-H), 6.88 (d, 1H, *J* = 4.9 Hz, Ar-H), 6.63-6.60 (m, 1H, Ar-H), 3.90 (s, 2H, CH₂); ¹³C NMR (75

MHz, DMSO- d_6): δ 172.2, 159.7, 148.7, 145.6, 145.4, 133.6, 132.3, 131.9, 131.6, 114.0, 113.6, 112.6, 38.5. Analysis. Calcd. for $C_{15}H_{12}BrN_3O_3$ (361.01): C, 49.74; H, 3.34; N, 11.60. Found: C, 49.61; H, 3.27; N, 11.39.

***N'*-(3-Nitrobenzylidene)-2-(4-bromophenyl)acetohydrazide (4o)**

The general experimental procedure described above afforded **4o** as a light brown solid (84%, 303 mg). m.p 210-211 °C; R_f : 0.78 (10% MeOH/ $CHCl_3$); IR (ATR, cm^{-1}): 3191 (NH), 3057 (Ar-H), 1666 (C=O), 1610 (C=N), 1552, 1525 (C=C); 1H NMR (300 MHz, DMSO- d_6): δ 11.38 (s, 1H, NH), 8.24-8.19 (m, 2H, Ar-H), 8.15 (s, 1H, C-H), 8.05-8.01 (m, 2H, Ar-H), 7.88-7.71 (m, 4H, Ar-H), 3.92 (s, 2H, CH_2); ^{13}C NMR (75 MHz, DMSO- d_6): δ 171.2, 152.2, 148.7, 142.5, 138.8, 135.1, 132.3, 131.8, 131.4, 131.5, 128.5, 128.3, 37.6. Analysis Calcd. for $C_{15}H_{12}BrN_3O_3$ (361.01): C, 49.74; H, 3.34; N, 11.60. Found: C, 49.58; H, 3.39; N, 11.42.

2-(4-Bromophenyl)-*N'*-(2-phenylpropylidene)acetohydrazide (4p)

The general experimental procedure described above afforded **4p** as a white solid (78%, 268 mg). m.p 160-161 °C; R_f : 0.75 (10% MeOH/ $CHCl_3$); IR (ATR, cm^{-1}): 3201 (NH), 3045 (Ar-H), 1657 (C=O), 1608 (C=N), 1629, 1587, 1556 (C=C); 1H NMR (300 MHz, DMSO- d_6): δ 11.25 (s, 1H, NH), 7.61 (s, 1H, C-H), 7.51-7.47 (m, 2H, Ar-H), 7.40-7.31 (m, 2H, Ar-H), 7.26-7.19 (m, 5H, Ar-H), 3.83 (s, 2H, CH_2), 3.71-3.67 (m, 1H, C-H), 1.38 (d, 3H, J = 6.6 Hz, CH_3); ^{13}C NMR (75 MHz, DMSO- d_6): δ 172.0, 166.3, 153.6, 143.0, 132.1, 131.8, 131.6, 129.2, 127.9, 127.2, 42.5, 19.1, 18.9. Analysis Calcd. for $C_{17}H_{17}BrN_2O$ (344.05): C, 59.14; H, 4.96; N, 8.11. Found: C, 59.02; H, 4.85; N, 8.24.

***N'*-(Biphenyl-4-ylmethylene)-2-(4-bromophenyl)acetohydrazide (4q)**

The general experimental procedure described above afforded **4q** as an off-white solid (79%, 310 mg). m.p 213-214 °C; R_f : 0.75 (10% MeOH/ $CHCl_3$); IR (ATR, cm^{-1}): 3179 (NH), 3022 (Ar-H),

1667 (C=O), 1639 (C=N), 1591, 1551 (C=C); ^1H NMR (300 MHz, DMSO- d_6): δ 11.70 (s, 1H, NH), 8.25 (s, 1H, C-H), 7.80-7.70 (m, 4H, Ar-H), 7.54-7.45 (m, 4H, Ar-H), 7.41-7.36 (m, 2H, Ar-H), 7.31-7.27 (m, 3H, Ar-H), 4.00 (s, 2H, CH₂); ^{13}C NMR (75 MHz, DMSO- d_6): δ 172.4, 166.6, 146.7, 143.1, 139.8, 135.7, 132.2, 131.9, 131.6, 131.5, 129.5, 128.3, 127.8, 127.1, 38.8. Analysis Calcd. for C₁₈H₁₇BrN₂O₂ (392.05): C, 57.92; H, 4.59; N, 7.51. Found: C, 57.86; H, 4.54; N, 7.29.

2-(4-Bromophenyl)-N'-(furan-2-ylmethylene)acetohydrazide (4r)

The general experimental procedure described above afforded **4r** as a white solid (85%, 260 mg). m.p 185-186 °C; R_f: 0.71 (10% MeOH/CHCl₃); IR (ATR, cm⁻¹): 3173 (NH), 3054 (Ar-H), 1659 (C=O), 1587 (C=N), 1538, 1514 (C=C); ^1H NMR (300 MHz, DMSO- d_6): δ 11.34 (s, 1H, NH), 8.45 (s, 1H, C-H), 7.98-7.92 (m, 3H, Ar-H), 7.47-7.38 (m, 2H, Ar-H), 7.10-7.04 (m, 2H, Ar-H), 3.83 (s, 2H, CH₂); ^{13}C NMR (75 MHz, DMSO- d_6): δ 171.2, 153.3, 146.6, 142.8, 139.9, 134.6, 132.5, 131.7, 131.5, 131.4, 38.6. Analysis Calcd. for C₁₃H₁₁BrN₂O₂ (306.00): C, 50.84; H, 3.61; N, 9.12. Found: C, 50.78; H, 3.49; N, 9.04.

2-(4-Bromophenyl)-N'-pentylideneacetohydrazide (4s)

The general experimental procedure described above afforded **4s** as a light yellow solid (74%, 219 mg). m.p 119-120 °C; R_f: 0.74 (10% MeOH/CHCl₃); IR (ATR, cm⁻¹): 3211 (NH), 3068 (Ar-H), 1669 (C=O), 1626 (C=N), 1589, 1552 (C=C); ^1H NMR (300 MHz, DMSO- d_6): δ 11.28 (s, 1H, NH), 7.98 (s, 1H, C-H), 7.78-7.75 (m, 2H, Ar-H), 7.40-7.31 (m, 2H, Ar-H), 3.84 (s, 2H, CH₂), 1.98-1.95 (m, 2H, CH₂), 1.33-1.29 (m, 4H, CH₂), 0.98 (t, 3H, J = 6.9 Hz, CH₃); ^{13}C NMR (75 MHz, DMSO- d_6): δ 172.6, 153.6, 132.5, 131.8, 131.4, 131.1, 44.4, 33.2, 30.5, 28.9, 20.8. Analysis Calcd. for C₁₃H₁₇BrN₂O (296.05): C, 52.54; H, 5.77; N, 9.43. Found: C, 52.63; H, 5.56; N, 9.32.

Biological protocol

Cell transfection with human alkaline phosphatases and protein sample preparation

COS-7 cells were transfected with plasmids expressing human APs (TNAP, PLAP, IAP, and GCAP)³² in 10-cm plates, by using Lipofectamine. The confluent cells were then incubated for 5 h at 37 °C in DMEM/F-12 in the absence of fetal bovine serum and with 6 µg of plasmid DNA and 24 µL of Lipofectamine reagent. The same volume of DMEM/F-12 containing 20% FBS was added to stop the transfection and the cells were harvested 48–72 h later.

The transfected cells were washed three times at 4 °C, with Tris–saline buffer, collected by scraping in the harvesting buffer (95 mM NaCl, 0.1 mM PMSF, and 45 mM Tris buffer, pH 7.5) and washed twice by centrifugation at 300g for 5 min at 4 °C.³³ Subsequently, cells were allowed to resuspend in the harvesting buffer containing 10 µg/mL aprotinin and sonicated. Cellular and nuclear debris were discarded by 10 min centrifugation (300×g at 4 °C). Glycerol was added (final concentration of 7.5%) to the resulting supernatant and the samples were kept at –80 °C until used. Protein concentration was determined by the Bradford microplate method and bovine serum albumin was used as a reference standard.³²

Alkaline phosphatase inhibition assay

A chemiluminescent substrate, CDP-star with or without tested inhibitors, was used for the determination of AP activity. For this the recombinant form of the following enzymes expressed in COS-7 cells as before^{32,33} were prepared: TNAP, IAP, PLAP and GCAP.^{6,18} The conditions for the assay were optimized with the slight modifications in previously used spectrophotometric method.²⁷ The assay buffer was composed of 2.5 mM MgCl₂, 0.05 mM ZnCl₂ and 8 M DEA (pH 9.8). The compounds were tested initially at the final concentration of 200 µM. The total volume of 50 µL contained 10 µL of each tested compound (final 200 µM with DMSO 1% (v/v)),

followed by the addition of 20 μL of h-TNAP (from 2.29 $\mu\text{g}/\text{mL}$ enzyme in assay buffer), 20 μL of h-IAP (from 2.84 $\mu\text{g}/\text{mL}$ enzyme in assay buffer), 20 μL of h-PLAP (from 3.0 $\mu\text{g}/\text{mL}$ enzyme in assay buffer) and 20 μL of h-GCLP (2.92 $\mu\text{g}/\text{mL}$ enzyme in assay buffer), in respective enzyme assay. The mixture was pre-incubated for 5–7 minutes at 37 $^{\circ}\text{C}$ and luminescence was measured as pre-read using microplate reader (BioTek FLx800, Instruments, Inc. USA). Then, in the respective enzymatic assay, 20 μL of CDP-star (final concentration of 110 μM) was added to initiate the reaction and the assay mixture was incubated again for 15 min at 37 $^{\circ}\text{C}$. The change in the luminescence was measured as after-read. The activity of each compound was compared with total activity control (without any inhibitor). Levamisole (0.2 mM per well) was used as a positive control for both the h-TNAP and h-PLAP isozymes. While, L-phenylalanine (0.4 mM per well) was used as a positive control for h-IAP. The compounds which exhibited over 50% inhibition of either of the above mentioned enzymes were further evaluated for determination of IC_{50} values. For this purpose serial dilutions of each compound were prepared in assay buffer and their dose response curves were obtained by assaying each inhibitor concentration against all APs using the above mentioned reaction conditions. All experiments were repeated in triplicate. The Cheng Prusoff equation was used to calculate the IC_{50} values, determined by the non-linear curve fitting program PRISM 5.0 (GraphPad, San Diego, California, USA).

Homology modelling and molecular docking studies

Using Modeller v9.14²⁸ via Chimera v1.10.1,²⁹ homology modelling of human derived germ cells alkaline phosphatase was carried out. Suitable target sequence of h-GCAP (Uniprot ID P10696) was identified using NCBI protein database and was fetched into Chimera v.1.10.1.²⁹ To identify suitable template structure, Basic Local Alignment Search Tool (BLAST) of NCBI was used. Crystal structures of human derived placental alkaline phosphatase was found to be the

most top ranking template structures. Crystal structure of human derived placental alkaline phosphatase PDB ID 1ZED was fetched into chimera and was added to the template query using Needleman Wunsch method. Homology modelling of the h-GCAP was then carried out using Modeller v9.14.²⁸ The top ranking model was then refined by adding hydrogens, Gasteiger charges and by completing the incomplete side chains using Dunbrack rotamer library³⁴ of Chimera v1.10.1. The overall quality of the homology models generated was then evaluated by Molprobit³⁵ and Ramachandran plot was plotted.

Chemical structures of potent inhibitors **4g**, **4k** and **4p** for docking inside the active site of h-PLAP, h-IAP and h-TNAP respectively, were drawn using ACD/ChemSketch,³⁶ structures were then 3D optimized. The chemical structures were saved in mol2 file format for subsequent recognition and docking.

Molecular docking calculations were carried out using FlexX utility of LeadIT from BioSolveIT GmbH, Germany.³⁷ Crystal Structure of h-PLAP (PDB ID 1ZED) was downloaded from RSC Protein Data Bank and homology models of h-TNAP and h-IAP previously modelled²⁴ and h-GCAP modelled now, was used for molecular docking studies. Prior to the performance of docking studies the receptor active site was defined as the amino-acid residues in 7.5 Å radius around the co-crystallized or modelled phosphate ions. Additionally, metal ions including two zinc metal ions and a magnesium metal ion bearing a charge of +2 respectively, was selected as part of the active site. Default parameters of amino acid flips, metal co-ordinates and solvent handling were used. Molecular docking of compounds were then carried out using default docking parameters and 50 top ranking poses were retained for visual inspection in Discovery Studio Visualizer³⁸ to determine the putative binding mode.

Acknowledgements

We thank the University of Otago for purchase of the diffractometer. J. Iqbal is thankful to the Organization for the Prohibition of Chemical Weapons (OPCW), The Hague, The Netherlands and Higher Education Commission of Pakistan for the financial support through Project No. 20-3733/NRPU/R&D/14/520. We are grateful to Prof. Dr. José Luis Millán for providing plasmids encoding APs. J. Sévigny received support from the Canadian Institutes of Health Research (CIHR) and he was also the recipient of a “Chercheur National” research award from the Fonds de recherche du Québec – Santé (FRQS).

Supplementary material

CCDC 1401865 (**4i**) and 1401866 (**4q**) contain the supplementary crystallographic data for this paper. These data can be obtained free of charge from The Cambridge Crystallographic Data Centre *via* http://www.ccdc.cam.ac.uk/data_request/cif.

References

1. R.B. McComb, G. N. Bowers and S. Posen, *Alkaline phosphatase*. New York: Plenum Press; 1979.
2. J.L. Millan, *Purinergic Signal.*, 2006, **2**, 335–341.
3. M. al-Rashida and J. Iqbal, *Med. Res. Rev.*, 2014, **34**, 703–743.
4. (a) M. Lanier, E. Sergienko, A.M. Simao, Y. Su, T. Chung, J. L. Millan and J.R. Cashman, *Bioorg. Med. Chem.*, 2009, **18**, 573–579; (b) E. A. Sergienko and J.L. Millan, *Nat. Protoc.*, 2010, **5**, 1431–1439.
5. J.L. Millán, *Mammalian Alkaline Phosphatases: From Biology to Applications in Medicine and Biotechnology*; Wiley-VCH: Weinheim, Germany, 2006.
6. (a) S. Sidique, R. Ardecky, Y. Su, S. Narisawa, B. Brown, J.L. Millán, E. Sergienko and N.D.P. Cosford, *Bioorg. Med. Chem. Lett.*, 2009, **19**, 222–225; (b) R. Dahl, E.A. Sergienko, Y.

- Su, Y.S. Mostofi, L. Yang, A.M. Simão, S. Narisawa, B. Brown, A. Mangravita-Novo, M. Vicchiarelli, L.H. Smith, W.C. O'Neill, J.L. Millán and N.D. Cosford, *J. Med. Chem.*, 2009, **52**, 6919–6925; (c) L. Li, L. Chang, S. Pellet-Rostaing, F. Liger, M. Lemaire, R. Buchet and Y. Wu, *Bioorg. Med. Chem.*, 2009, **17**, 7290–7300; (d) C.R. Sheen, P. Kuss, S. Narisawa, M.C. Yadav, J. Nigro, W. Wang, T.N. Chlea, E. Sergienko, K. Kapoor, M.R. Jackson, M.F. Hoylaerts, A.B. Pinkerton, W.C. O'Neill and J.L. Millán, *J. Bone Miner. Res.*, 2015, **30**, 824–836.
7. L. Fishman, H. Miyayama, S. G. Driscoll and W.H. Fishman, *Cancer Res.*, 1976, **36**, 2268–2273.
8. (a) W.H. Fishman, N.K. Ghosh, N.R. Inglis and S. Green, *Enzymologia*, 1968, **34**, 317–321; (b) W.H. Fishman, N.R. Inglis, S. Green, C.L. Anstiss, N.K. Gosh, A.E. Reif, R. Rustigian, M.J. Krant and L.L. Stolbach, *Nature*, 1968, **219**, 697–699.
9. C.M. Povinelli and B.J. Knoll, *Placenta*, 1991, **12**, 663–668.
10. (a) B. Wahren, P.A. Holmgren and T. Stigbrand, *Int. J. Cancer*, 1979, **24**, 749–753; (b) B. Wahren, J. Hinkula, T. Stigbrand, A. Jeppsson, L. Andersson, P.L. Esposti, F. Edsmyr and J.L. Millán, *Int. J. Cancer*, 1986, **37**, 595–600.
11. K.A. Smans, M.B. Ingvarsson, P. Lindgren, S. Canevari, H. Walt, T. Stigbrand, T. Bäckström and J.L. Millán, *Int. J. Cancer*, 1999, **83**, 270–277.
12. C.E. Ovitt, A.W. Strauss, D.H. Alpers, J.Y. Chou and I. Boime, *Proc. Natl. Acad. Sci. U.S.A.*, 1986, **83**, 3781–3785.
13. (a) S. Narisawa, L. Huang, A. Iwasaki, H. Hasegawa, D.H. Alpers and J.L. Millán, *Mol. Cell Biol.*, 2003, **23**, 7525–7530; (b) T. Nakano, I. Inoue, I. Koyama, K. Kanazawa, K. Nakamura, S. Narisawa, K. Tanaka, M. Akita, T. Masuyama, M. Seo, S. Hokari, S. Katayama, D.H. Alpers, J. L. Millán and T. Komoda, *Am. J. Physiol. Gastrointest. Liver Physiol.*, 2007, **292**, 1439–1449.

14. R.F. Goldberg, W.G. Austen Jr, X. Zhang, G. Munene, G. Mostafa, S. Biswas, M. McCormack, K.R. Eberlin, J.T. Nguyen, H.S. Tatlidede, H.S. Warren, S. Narisawa, J.L. Millán and R.A. Hodin, *Proc. Natl. Acad. Sci. USA.*, 2008, **105**, 3551–3556.
15. S. Narisawa, M.F. Hoylaerts, K.S. Doctor, M.N. Fukuda, D. H. Alpers and J.L. Millán, *Am. J. Physiol. Gastrointest. Liver Physiol.*, 2007, **293**, 1068–1077.
16. (a) W.H. Fishman and H.G. Sie, *Enzymologia*, 1971, **41**, 141–167; (b) G.J. Doellgast and W.H. Fishman, *Clin. Chim. Acta*, 1977, **75**, 449–454.
17. C.W. Lin and W.H. Fishman, *J. Biol. Chem.*, 1972, **247**, 3082–3087.
18. R.J. Ardecky, E.V. Bobkova, T. Kiffer-Moreira, B. Brown, S. Ganji, J. Zou, I. Pass, S. Narisawa, F.G. Iano, C. Rosenstein, A. Cheltsov, J. Rascon, M. Hedrick, C. Gaslor, A. Forster, S. Shi, R. Dahl, S. Vasile, Y. Su, E. Sergienko, T.C. Chung, J. Kaunitz, M.F. Hoylaerts, A.B. Pinkerton and J.L. Millán, *Bioorg. Med. Chem. Lett.*, 2014, **24**, 1000–1004.
19. K. Padmini, P.J. Preethi, M. Divya, P. Rohini, M. Lohita, K. Swetha and P. Kaladar, *Int. J. Pharm. Res. Rev.*, 2013, **2**, 43–58.
20. C. A. Fraga and E.J. Barreiro, *Curr. Med. Chem.*, 2006, **13**, 167–198; (b) E.H. Anouar, S. Raweh, I. Bayach, M. Taha, M.S. Baharudin, F.D. Meo, M.H. Hasan, A. Adam, N.H. Ismail, J. F. Weber and P. Trouillas, *J. Comput. Aided Mol. Des.*, 2013, **27**, 951–964; (c) M. Taha, M.S. Baharudin, N.H. Ismail, K.M. Khan, F.M. Jaafar, S. S. Siddiqui and M.I. Choudhary, *Bioorg. Med. Chem. Lett.*, 2013, **23**, 3463–3466; (d) M. Taha, N.H. Ismail, W. Jamil, S. Yousuf, F.M. Jaafar, M.I. Ali, S. M. Kashif and E. Hussain, *Molecules*, 2013, **18**, 10912–10929.
21. S.G. Musharraf, A. Bibi, N. Shahid, M.N.U.H. Khan, M. Taha, U. R. Mughal and K.M. Khan, *Am. J. Anal. Chem.*, 2012, **3**, 779–789.

22. W.B. Júnior, M.S. Alexandre-Moreira, M.A. Alves, A. Perez-Rebolledo, G.L. Parrilha, E.E. Castellano, O.E. Piro, E.J. Barreiro, L.M. Lima and H. Beraldo, *Molecules*, 2011, **16**, 6902–6915.
23. P. Diaz, J. Xu, F. Astruc-Diaz, H.M. Pan, D.L. Brown and M. Naguib, *J. Med. Chem.*, 2008, **51**, 4932–4947.
- 24.(a) M. al-Rashida, R. Raza, G. Abbas, M.S. Shah, G.E. Kostakis, J. Lecka, J. Sévigny, M. Muddassar, C. Papatriantafyllopoulou and J. Iqbal, *Eur. J. Med. Chem.*, 2013, **66**, 438–449; (b) M. al-Rashida, S.A. Ejaz, S. Ali, A. Shaukat, M. Hamayoun, M. Ahmed and J. Iqbal, *Bioorg. Med. Chem.*, 2015, **23**, 2435–2444; (c) I. Khan, S.J.A. Shah, S.A. Ejaz, A. Ibrar, S. Hameed, J. Lecka, J.L. Millan, J. Sévigny and J. Iqbal, *RSC Adv.*, 2015, **5**, 64404–64413.
25. (a) I. Khan, A. Ibrar and J.M. White, *Crystals*, 2012, **2**, 521–527; (b) I. Khan, S. Ali, S. Hameed, N.H. Rama, M.T. Hussain, A. Wadood, R. Uddin, Z. Ul-Haq, A. Khan, S. Ali and M.I. Choudhary, *Eur. J. Med. Chem.*, 2010, **45**, 5200–5207; (c) I. Khan, M. Hanif, A.A. Khan, N.H. Rama, M.T. Hussain, M.A. S. Aslam and J. Iqbal, *Aust. J. Chem.*, 2012, **65**, 1413–1419; (d) M. Hanif, I. Khan, N.H. Rama, S. Noreen, M.I. Choudhary, P. G. Jones and M. Iqbal, *Med. Chem. Res.*, 2012, **21**, 3885–3896.
26. L.N.F. Cardoso, M.L.F. Bispo, C.R. Kaiser, J.L. Wardell, S.M.S.V. Wardell, M.C.S. Lourenço, F.A.F.M. Bezerra, R.P.P. Soares, M.N. Rocha and M.V.N. de Souza, *Arch. Pharm. Chem. Life Sci.*, 2014, **346**, 1–17.
27. E.A. Sergienko and J.L. Millán. *Nat. Protoc.*, 2010, **5**, 1431–1439.
28. A. Sali and T.L. Blundell, *J. Mol. Biol.*, 1993, **234**(3), 779–815.
29. E.F. Pettersen, T.D. Goddard, C.C. Huang, G.S. Couch, D.M. Greenblatt, E.C. Meng and T.E. Ferrine, *J. Comput. Chem.*, 2004, **25**, 1605–1612.

30. M.-H. Le Du and J.L. Millán, *J. Biol. Chem.*, 2002, **277**(51), 49808–49814.
31. N. Sakai, T. Moriya and T. Konakahara, *J. Org. Chem.*, 2007, **72**, 5920–5922; (b) D. Dorsch, O. Schadt, F. Stieber and A. Blaukat, *US patent* 8,497,266 B2, Jul. 30, 2013.
32. (a) F. Kukulski, S.A. Lévesque, E.G. Lavoie, J. Lecka, F. Bigonnesse, A.F. Knowles, S.C. Robson, T.L. Kirley and J. Sévigny, *Purinergic Signal.*, 2005, **1**, 193–204. (b) S. Narisawa, D. Harmey, M.C. Yadav, W.C. O'Neill, M. F. Hoylaerts and J.L. Millán, *J. Bone Miner. Res.*, 2007, **22**, 1700–1710. (c) M.M. Bradford, *Anal. Biochem.*, 1976, **72**(1), 248–254
33. T. Kiffer-Moreira, C.R. Sheen, K.C. da Silva Gasque, M. Bolean, P. Ciancaglioni, A. van Elsas, M.F. Hoylaerts and J.L. Millán, *PLoS ONE*, 2014, **9**(2), e89374.
34. R.L. Dunbrack, *Curr. Opin. Struct. Biol.*, 2002, **12**, 431–440.
35. V.B. Chen, W.B. 3rd Arendall, J.J. Headd,; D.A. Keedy, R.M. Immormino, G.J. Kapral, L.W. Murray, J.S. Richardson, D.C. Richardson, *Acta Crystallogr. D Biol. Crystallogr.*, 2010, **66**, 12–21.
36. O. Toronto, Canada Advanced Chemistry Development, Inc. Acd/chemsketch (freeware), version 12.01. 2009.
37. LeadIT, B., <http://www.biosolveit.de/LeadIT>. accessed 12th Mar, 2011.
38. D.S. Visualiser, 2.5. 1, Accelrys Software Inc. Discovery Studio Modeling Environment, Release. 2.